A statistical shape model for estimating missing soft tissues of the face in a black South African population

Helene Francia Swanepoel MSc [1,*], Harold S. Matthews PhD [2,3,4], Peter Claes PhD [2,3,4,5], Dirk Vandermeulen PhD [3,5], Anna C. Oettlé MD, PhD [1,6]

[1] Department of Anatomy, University of Pretoria, Pretoria, South Africa
[2] Laboratory for Imaging Genetics, Department of Human Genetics, Katholieke Universiteit, Leuven, Belgium
[3] Medical Imaging Research Center, Universitair Ziekenhuis, Leuven, Belgium
[4] Facial Sciences, Murdoch Children's Research Institute, Parkville, Australia
[5] Department of Electrical Engineering, Katholieke Universiteit, Leuven, Belgium
[6] Anatomy and Histology Department, Sefako Makgatho Health Sciences University, Pretoria, South Africa

*Correspondence: Helene Francia Swanepoel, 11 Northfields Avenue, Gwynneville, NSW, 2500, Australia. Email: u27089691@tuks.ac.za

Previous presentations: University of Cape Town Annual Face Science Symposium, Zoom virtual meeting, 8 November 2022.

Funding information
Bakeng se Afrika, Grant/Award Number: 597924-EPP-1-2018-1-ZA-EPPKA2-CBHE-JPrevious presentations: University of Cape Town Annual Face Science Symposium, Zoom virtual meeting, 8 November 2022.

ABSTRACT

Purpose: Facial disfigurement may affect the quality of life of many patients. Facial prostheses are often used as an adjuvant to surgical intervention and may sometimes be the only viable treatment option. Traditional methods for designing soft-tissue facial prostheses are time-consuming and subjective, while existing digital techniques are based on mirroring of contralateral features of the patient, or the use of existing feature templates/models that may not be readily available. We aim to support the objective and semi-automated design of facial prostheses with primary application to midline or bilateral defect restoration where no contralateral features are present. Specifically, we developed and validated a statistical shape model (SSM) for estimating the shape of missing facial soft tissue segments, from any intact parts of the face.

Materials and Methods: An SSM of 3D facial variations was built from meshes extracted from computed tomography and cone beam computed tomography images of a black South African sample (n = 235) without facial disfigurement. Various types of facial defects were simulated, and the missing parts were estimated automatically by a weighted fit of each mesh to the SSM. The estimated regions were compared to the original regions using color maps and root-mean-square (RMS) distances.

Results: Root mean square errors (RMSE) for defect estimations of one orbit, partial nose, cheek, and lip were all below 1.71 mm. Errors for the full nose, bi-orbital defects, as well as small and large composite defects were between 2.10 and 2.58 mm. Statistically significant associations of age and type of defect with RMSE were observed, but not with sex or imaging modality.

Conclusion: This method can support the objective and semi-automated design of facial prostheses, specifically for defects in the midline, crossing the midline or bilateral defects, by facilitating time-consuming and skill-dependent aspects of prosthesis design.

KEYWORDS : computer-aided design, facial prostheses, facial variation, midline defects, soft-tissue facial defects

The face is fundamental to human social interaction, among other functions. Even seemingly minor facial disfigurement may result in social anxiety, depression, and poor self-esteem, ultimately lowering quality of life.[1-4] Disfigurement may be the result of congenital deformities, infectious lesions (including fungal[5] and bacterial infections[6]), trauma, both human immunodeficiency virus (HIV)-related lesions like Kaposi's sarcoma and non-Hodgkin's lymphoma,[7] and non-HIV-related cancerous lesions, as well as conditions with complex pathology such as noma.[7-11] Additionally, the surgical resection of both cancerous and non-cancerous tumors often results in disfigurement.[12]

The rehabilitation of facial defects continues to need complex interventions. Despite advances in surgical rehabilitation techniques, limiting factors include inadequate residual soft and hard tissue and vascular compromise following radiation exposure.[13] The restoration of ocular loss continues to lack a viable solution. The surgical reconstruction of ear[14] and nose[15] defects also presents unique challenges. Successfully addressing defects of these features by accurately replicating their intricate three-dimensional geometry requires complex surgical techniques and the availability of appropriate donor tissues.[16, 17]

Over the past two decades, facial transplantation has emerged as an effective treatment for patients burdened with extensive facial disfigurement, particularly when autologous strategies fail to restore optimal facial form and function. This approach, however, is still not widely performed and has stringent criteria to be met before consideration.[18] When the functional and aesthetic requirements are beyond the capacity of local reconstructive efforts, aesthetic prostheses are an alternative or adjunct rehabilitation option, especially for older patients or those with significant comorbidities.[13, 19, 20] From a biopsychosocial perspective, facial prostheses have been shown to improve severe functional, cognitive, and aesthetic impairments caused by facial deformities, thereby positively impacting patients' daily lives and well-being.[21]

Although the most recent prevalence figures regarding facial disfigurements in patients requiring prostheses in South Africa date back to 2001, they emphasize that facilities, budgets, and staff were not sufficient to address the growing need for prosthetic care in the South African context,[22] where this study was based. Currently, with high prevalence rates of conditions associated with facial disfigurement, such as cancer,[23] HIV,[24] noma,[8, 9] and facial

trauma,[25] there is an increasing demand for alternative and adjunct rehabilitation options. The body of literature concerning facial prosthetics in South Africa is predominantly composed of case studies, lacking a targeted examination of the accuracy or efficacy of facial restoration techniques. A combination of artistic methods is employed to design and manufacture facial prostheses, which can be time- and energy-intensive and rely significantly on artistic skills. Unfortunately, there is a relative shortage of both training facilities and trained technicians capable of performing these tasks.[26] Furthermore, as of 2021, there were only 83 prosthodontists practicing in the whole of South Africa.[27] With the need for facial prostheses exceeding what can be offered by oral health facilities and workers and the unequal distribution of services in the country,[26, 28] delays in producing facial prostheses may result and contribute to extensive waiting lists for patients in need of rehabilitation.

Objective and automated methods for designing facial prostheses could substantially reduce the time cost and waiting times. For unilateral defects, computerized methods based on mirroring the intact half of the face about the midline are used in the design of prostheses.[29] The mirroring approach, while ideal for unilateral defects is not as effective and often cannot be applied at all to defects that cross the facial midline or to bi-lateral defects. Statistical shape models (SSMs) are a concise mathematical description of the variation within a sample of homologous objects, comprising the mean shape and the principal modes of variation from the mean.[30, 31] In contrast to the mirroring approach, by using an SSM, missing parts of a shape can be inferred from any available intact parts, not only regions bilaterally paired with the defect. SSMs have been applied for the reconstruction of pelvic defects,[32] mandibular defects,[33] orbital floor defects,[34] and reconstructions of cranial vault and midfacial (skeletal) defects.[35, 36]

In this study, facial variation among black South Africans was modeled by means of an SSM, and the use of this SSM was evaluated to mathematically estimate missing soft tissue parts for a sample of artificially defective faces. This tool can contribute to the design and manufacturing of aesthetic prostheses by establishing a more objective and semi-automated approach to estimating missing soft tissue segments of the face and is particularly valuable for bi-lateral defects and defects that cross the facial midline, where mirroring techniques cannot be applied. Furthermore, this study seeks to expand the existing scientific discourse by integrating empirical findings specifically related to individuals of African descent.

MATERIALS AND METHODS

Ethical approval for this study was obtained from the Faculty of Health Sciences Ethics Committee at the University of Pretoria (Ref# 58/2020). A sample comprising cone beam computed tomography (CBCT) and computed tomography (CT) images of adult black South African patients were retrospectively collected from two private and one state-owned health care facilities in Pretoria, South Africa. All identifying metadata was removed, with only age and sex recorded. Scans were excluded if the face showed any underlying pathology, evidence of current orthodontic treatment, or visible facial interventions. The sample comprised 118 CBCT (age range: 18–87) and 119 CT (age range: 18 - 85) scans. The demographic characteristics of the sample are shown in Table 1.

TABLE 1. Demographics of the sample.

		CBCT (*n* = 118)										CT (*n* = 119)									
		Male					Female					Male					Female				
		Total (n = 64)	With Chins[a] (n = 0)	Open eyes (n = 44)	Incl. in Model Training Dataset (n = 37)	Incl. in Defect Dataset (n = 8)	Total (n = 54)	With Chins[a] (n = 1)	Open eyes (n = 29)	Incl. in Model Training Dataset (n = 33)	Incl. in Defect Dataset (n = 7)	Total (n = 67)	With Chins[a] (n = 59)	Open eyes (n = 35)	Incl. in Model Training Dataset (n = 48)	Incl. in Defect Dataset (n = 7)	Total (n = 50)	With Chins[a] (n = 42)	Open eyes (n = 18)	Incl. in Model Training Dataset (n = 30)	Incl. in Defect Dataset (n = 8)
Age (years old)	18–30	**27**	0	18	**16**	**3**	**15**	0	9	**11**	**1**	**22**	19	10	**16**	**2**	**16**	13	7	13	1
	31–40	**19**	0	13	**10**	**2**	**12**	0	5	**8**	**1**	**18**	16	9	**15**	**1**	**18**	16	7	10	3
	41–50	**5**	0	4	**3**	**1**	**9**	0	7	**5**	**1**	**7**	7	4	**4**	**1**	**5**	5	1	0	1
	51–60	**9**	0	6	**7**	**0**	**9**	0	4	**4**	**2**	**6**	6	6	**2**	**1**	**5**	4	1	4	1
	60+	**4**	0	3	**1**	**2**	**9**	1	4	**5**	**2**	**4**	2	1	**1**	**2**	**5**	4	2	2	2
	Unknown	**0**	0	0	**0**	**0**	**0**	0	0	**0**	**0**	**10**	9	5	**10**	**0**	**1**	0	0	1	0

[a] Complete morphology of the chin is available, that is, a chin strut, as usually seen in CBCT[61], was not present.

An overview of the entire process of estimating missing soft tissue segments of the face is illustrated in Figure 1, including the creation of the SSM and how it is used to estimate defected regions of the face.

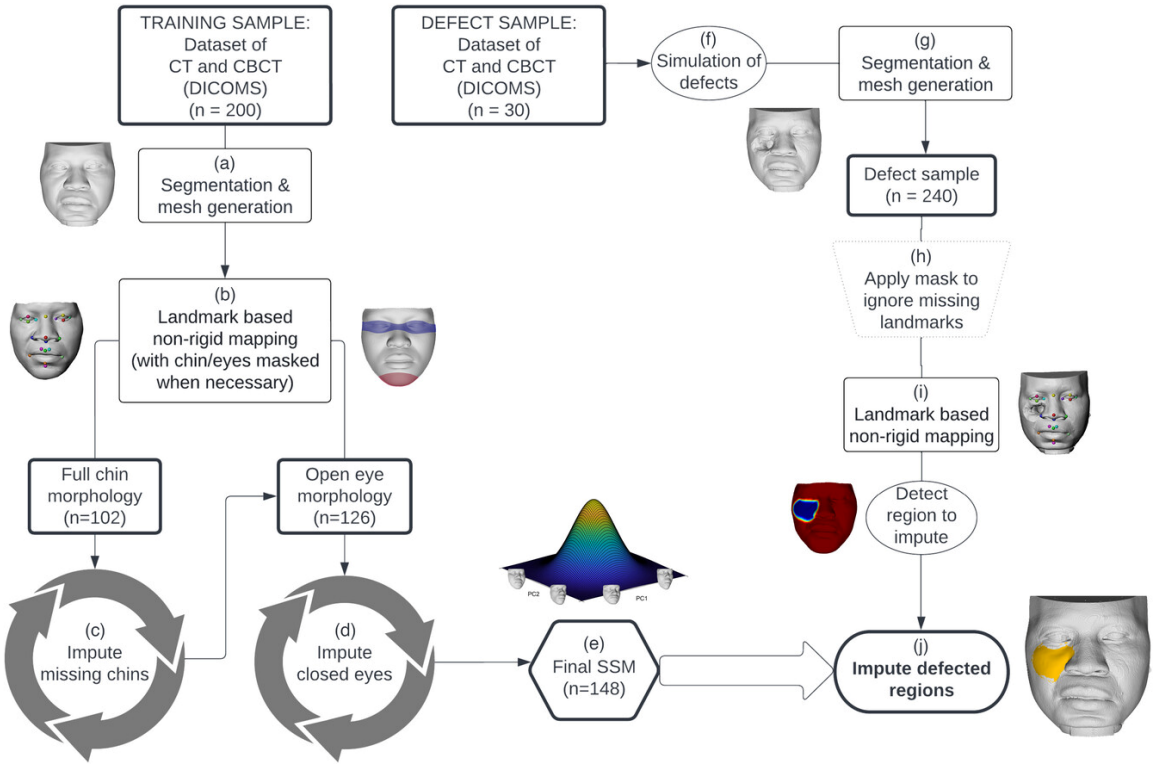

FIGURE 1. Methodology overview. The left side of the figure shows the steps involved in generating the statistical shape model used to estimate missing regions of the defective face. The right side of the figure shows the steps involved in creating a sample of simulated defects, mapping the defective sample, and using the SSM to estimate the defective regions. (a) A training set of DICOMS was segmented and the resulting iso-surface of the soft tissue face was tessellated into meshes for further processing. (b) To achieve correspondence, a set of 20 landmarks was placed on the meshes and a standard facial template. Non-rigid mapping was conducted in the MeshMonk toolbox to ensure a standardized topology across all meshes. (c) and (d) An iterative bootstrapping approach was followed to estimate chins and eyes for samples without complete chin morphology or with closed eyes and sequentially added to the SSM. (e) The final SSM was generated by calculating the modes of variation (through Principal Component Analysis) for the total sample including open eye and chin estimations. (f) Six classes of facial defects were simulated using the Avizo software. (g) Defect faces were segmented and tessellated into meshes for further processing. (h) Missing landmarks due to defect regions were masked from the subsequent mapping during (I) by assigning 'target flags'. (j) The defect regions were estimated using the SSM by the same process used to estimate the chins and eyes in (c) and (d) and visualized in the context of the original unprocessed defective mesh. A more detailed description of each step can be found in the Supplementary Materials sections 1.1 to 1.3.

Threshold segmentation of each CT and CBCT scan was performed to segment the soft tissue and support structures from the background of the image. The resulting iso-surface was tessellated into a mesh. Constructing an SSM and estimating missing parts of a shape from it requires that each face be represented by a mesh of the same number of vertices and that these vertices should correspond across all instances of the shapes. This was done by non-

rigidly registering (mapping) a standard facial template mesh onto all the meshes in the training sample (Supplementary methods 1.1.1) using the MeshMonk toolbox[37] (https://gitlab.kuleuven.be/mirc/meshmonk) in MATLAB.[38] An SSM of black South African faces was built (Figure 1a–e) (Supplementary methods 1.1.3) and evaluated (Supplementary methods 1.1.4) in terms of generalization and specificity. Generalization represents how well the model can represent realistic faces not used in training, while specificity concerns the ability of the SSM to represent only realistic or valid faces.[39] The defect sample comprised 240 simulated defects (Figure 1f, Supplementary methods 1.2) on 30 faces with open eyes, according to 6 classes (Table S1). Class 1 to 5 were individual feature defects of the orbital region, cheek and upper lip, lips or isolated lower lip, full nasal region, and partial nasal region, respectively. Class 6 defects involved more than one facial feature in assorted combinations. Large (composite 1) defects involved three features, e.g., orbital, cheek, and full nose defects; small (composite 2) defects involved two features e.g., partial nose and lips; and bi-orbital defects included defects in both eyes. The defect faces were then segmented and tessellated into a mesh (Figure 1g). Correspondence with the standard facial template was established (Figure 1i) for each original non-defective face, along with its defective copies, as described in the Supplementary methods section 1.1.1. The region of interest (area to be estimated) was identified on the unprocessed defective scan by manual selection (Supplementary methods 1.3) and then transferred onto the topology of the template and the SSM. It should be noted that in our sample of simulated defective faces, there was no fibrosis or scar tissue present. In a real clinical scenario, all abnormal tissues should be selected as the region of interest. The final SSM was used to estimate the linear combination of the modes of variation that most closely approximates the intact regions of each face by using a weighted projection of the modes of variation (Supplementary methods 1.1.3 and 1.3). The face reconstructed from these projections was blended with the mapped version of the defective face. This result is the mapped version of the defective face with vertices of the defective region substituted with those of the weighted fit face. The estimated region was then visualized and interpreted in the context of the original unprocessed defective mesh (qualitative evaluation) (Figure. 1j).

A quantitative evaluation of the defect estimations was also conducted. The error for each defected scan was quantified as the RMS distance between the original mapped scan without the defect and its estimation, computed over the estimated region. A linear mixed model assessed the contributions of demographic and imaging factors as well as the type of defect to the RMSE. Demographic and imaging factors all varied between subjects and included age, imaging modality (CT/CBCT), and sex (male/female). Defect type varied within subjects (orbital, cheek, lip, full nasal, partial nasal, bi-orbital, large composite, and small composite). The mixed model comprised fixed main effects of each factor and intercepts for each participant and was fitted using lmerTest package[40] in R.[41] Residuals were plotted against the fitted values and evaluated for heteroscedasticity, skewness, and kurtosis.

RESULTS

Quantitative evaluation of the defect estimations

Figure 2 shows the distribution of errors plotted by defect type, sex, imaging modality, and age. Means and standard deviations of the errors by defect type are also reported in Table 2. Errors for unilateral orbital defects, the partial nose, cheek, and lip were all below 1.71 mm.

Errors for the full nose, composite 1 (large—combination of three features) and composite 2 (small—combination of two features), and bi-orbital defects were between 2.10 and 2.58 mm.

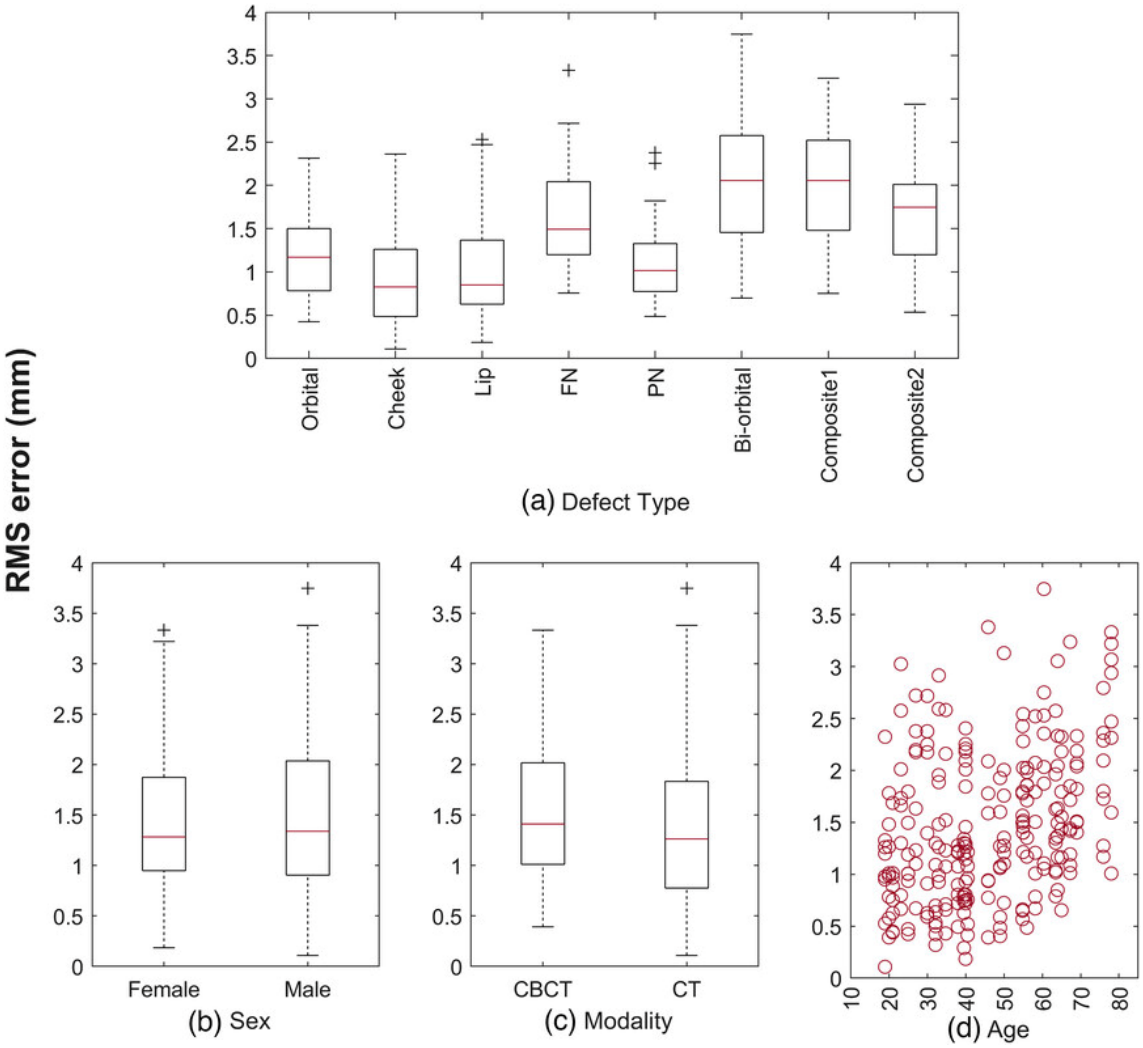

FIGURE 2. Accuracy of defect reconstructions. (a) RMSE for the different classes of defect, showing errors below 1.71 mm for all isolated feature defects except the full nose. Full nose, bi-orbital, and composite defects show slightly higher errors, all below 2.58 mm. (b) RMSE according to sex and (c) modality show no differences in reconstruction errors between male and female, or CBCT and CT, respectively. (d) RMSE according to age.

TABLE 2. RMS error for defect types in millimeters.

Defect type	Orbital	Cheek	Lip	FN	PN	Bi-orbital	Large Composite	Small Composite
Mean	1.71	1.43	1.54	2.10	1.63	2.58	2.48	2.14
SD	0.51	0.51	0.65	0.59	0.47	0.76	0.69	0.59

The linear mixed model showed main effects of age ($F(1,26) = 16.949$, $p < 0.001$) and defect type ($F(7,203) = 27.030$, $p < 0.001$) on RMSE were significant, all others were not ($p > 0.050$, Table S2). Residuals were plotted against the fitted values, and we found no evidence of heteroscedasticity. Residuals were normally distributed with low skewness (0.52) and kurtosis close to three (3.25). The unstandardized regression coefficient for age showed the effect is a small decrease in error of −0.015 mm (SE = 0.003) per year. The expected values and 95% confidence intervals of the expectation for each defect type are shown in Figure S1. From this and the boxplots in Figure 2 we see that the full nose and larger defects including bi-orbital and composites 1 and 2 are the most difficult to estimate.

Qualitative evaluation of the defect estimations

An example of defect estimations (a—h) for one sample is shown in Figure 3. Estimations of all defects were assessed visually by author HFS and rendered images of the CBCT sample can be found in the supplementary information (Figures S2–S16). In approximately 38% of cases, the defect was smoothly blended with the surrounding tissue. Cheek and full nose defects performed the best, with respectively 63 % and 60% of instances smoothly blending. Non-smooth blending (e.g., Figure 4) was most frequent for bi-orbital defects (87 %), followed by composite 1 (80 %), and, composite 2 and lip (both at 67%). As seen in Figure 4, the majority of these issues were due to the region selected for estimation being sub-optimal (see Supplementary results for more information). Thirteen cases of poor defect estimations were because of failed non-rigid registration. In 10 cases, the defects extended beyond the anatomical region covered by the facial template (Figure 5) and were thus incompletely estimated, only including the region covered by the template.

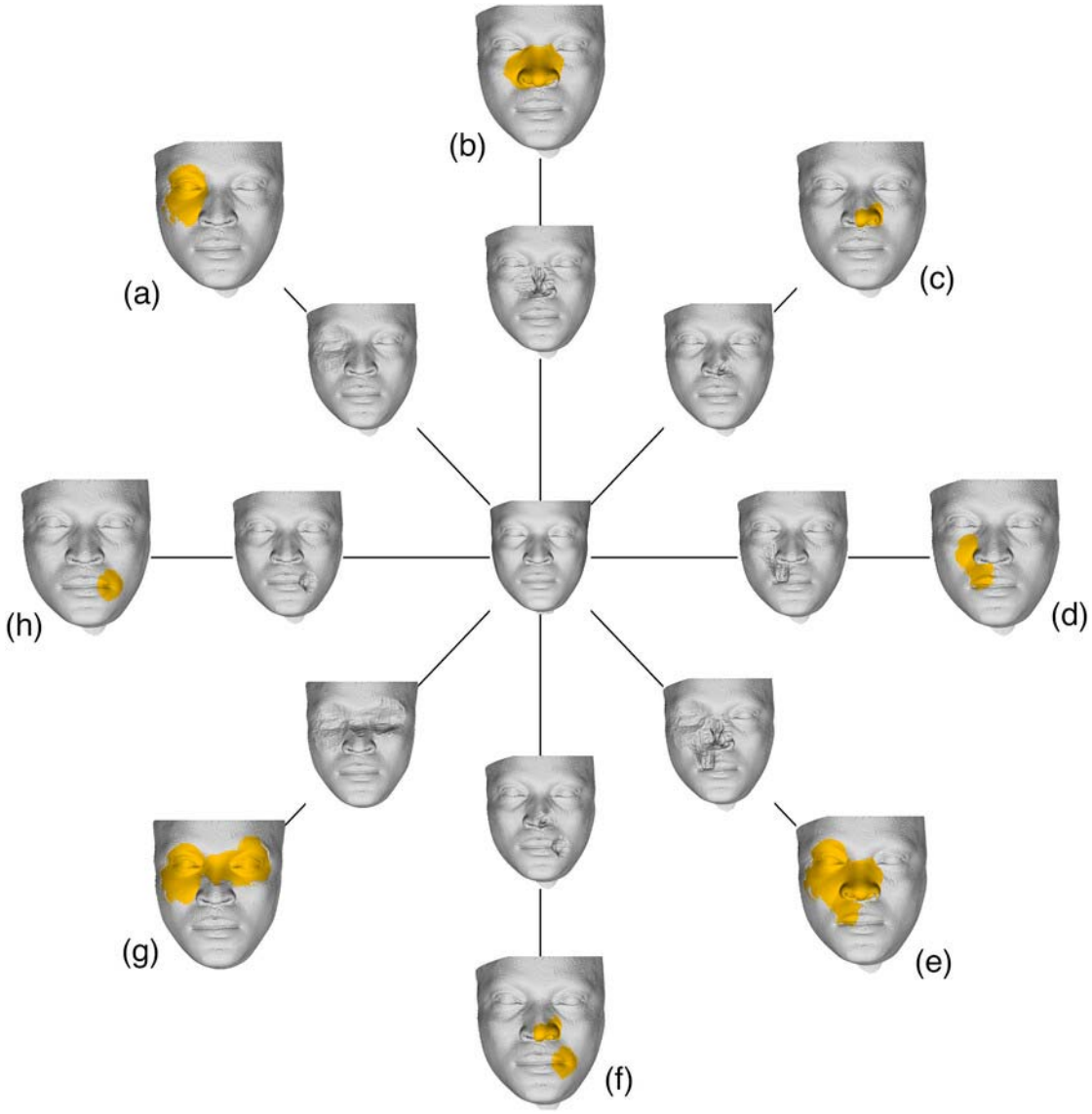

FIGURE 3. Example of one individual's defect estimations. The central image is the original non-defective face; the inner ring represents the different defect simulations; the outer ring shows in orange the defect estimation superimposed onto the defective face. (a) Orbital defect, (b) Full nose defect, (c) Partial nose defect, (d) Cheek defect, (e) Large (composite 1) defect, (f) Small (composite 2) defect, (g) Bi-orbital defect, and (h) Lip defect.

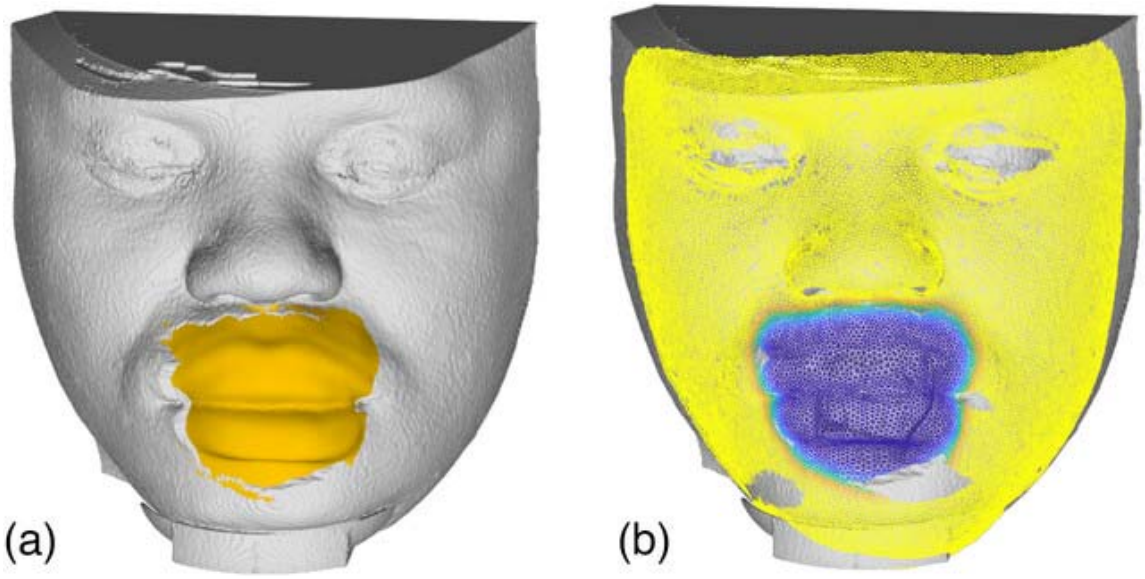

FIGURE 4. Example of a poor defect estimation of the lips. (a) The corners of the mouth and parts of the chin (in grey) are cut off due to the flagged defective region seen in blue in (b) being too small.

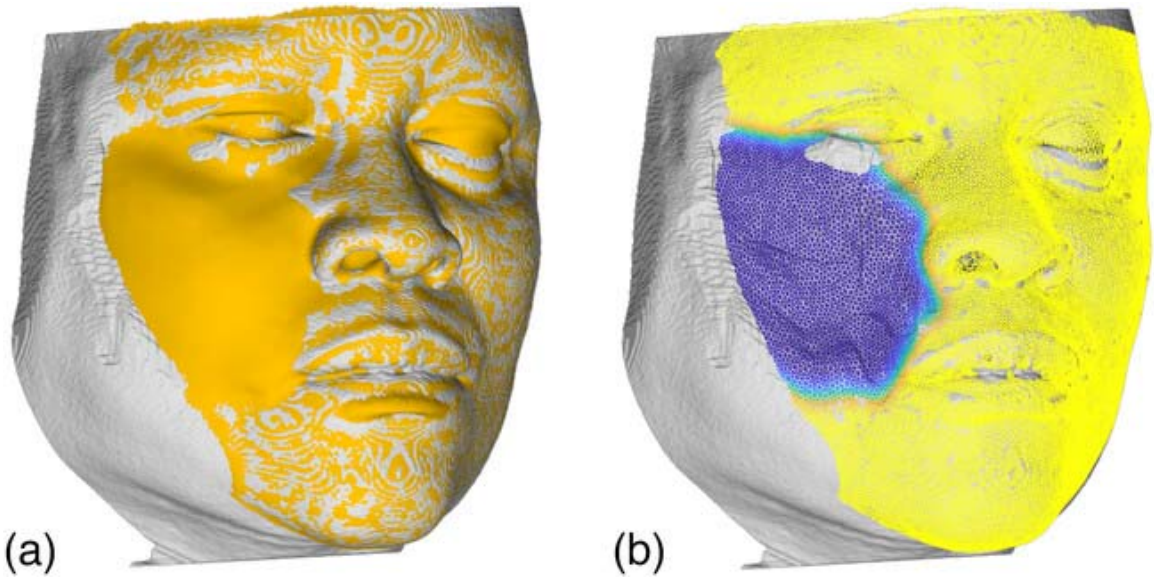

FIGURE 5. Example of mismatch between the region of the defect estimation and the original defective face due to the defect extending beyond the borders of the template. (a) The estimation (in orange) does not cover the defective region. (b) Mapping of the defective scan shows that the template does not capture the entire surface of the face, with the flagged defective region in blue.

DISCUSSION

In our study, we propose an alternative approach for designing facial prosthetics by evaluating the use of an SSM to infer the most statistically plausible missing regions based on real facial variation. Nowadays, the prosthetic rehabilitation of unilateral defects is easily approached by employing digital mirroring techniques,[42-49] however, midline and bilateral facial defects still present challenges in computer-aided design. Currently, the predominant approach to

these defects involves the use of templates or archetypes.[47, 50-53] While effective in reducing the treatment period and the intensity of work required by technicians,[53] this solution necessitates access to a digital library of facial feature templates—a resource that is not readily available. Furthermore, this approach remains time-consuming, as the operator needs to experiment with a variety of templates to find the most aesthetically pleasing one.[50]

The model we propose proved particularly useful in handling defects crossing the midline, such as the nose, mouth, and bilateral defects. It also showed a satisfactory ability to represent realistic faces, including those outside of the training sample. As anticipated, the accuracy of the model varied between defect types due to the degree of covariation between defective and intact regions. In other words, the strength of the linear relationship between the given defective and intact regions influences the accuracy of a specific estimation. While theoretically, any type or size of defect may be estimated, the accuracy depends on the degree of covariation as well as the particular subject's agreement with the population-level covariance pattern. While estimation errors were deemed acceptable throughout, it is noteworthy that the partial nose and unilateral orbital defects had particularly low errors and full nose and bi-orbital defects, though slightly higher, still fell well within acceptable error ranges. We identified no statistically significant differences in the accuracy of simulated defects estimation across sexes or imaging modalities. Moreover, we observed a subtle trend of decreasing error (−0.015 mm per year) with increasing age, suggesting that the SSM's accuracy improves slightly with older subjects. The overall error for the model is acceptable across the age range of the defective sample (19–78 years).

Our computerized method possesses several advantages over conventional ones, which are often labor-intensive for both the patient and the clinician. Designing and manufacturing a prosthesis entails three key stages: obtaining an impression of the face model, designing the prosthesis model, and manufacturing the prosthesis model.[54] By replacing the skill-dependent sculpting of the missing feature from wax with digital techniques, our approach may reconstruct the missing soft tissue more efficiently. A computerized approach dramatically reduces patient involvement by capturing facial anatomy using CT/CBCT/laser scanners, offering a less traumatic experience. Additionally, it enables digital storage of information for future use,[55] which proves beneficial when a prosthesis needs to be replicated due to wear and tear or silicone discoloration. A scanning approach mitigates the need for repeated measurements or manual production, and it addresses bias and subjectivity in the design process.[56, 57]

Despite these benefits, our method has certain limitations. In particular, the estimated region did not always blend smoothly with the adjacent soft tissue in some scenarios. This difficulty primarily stems from the imprecise selection of the estimated region, a challenging task to perfect across a broad sample of scans. In the future, a graphical user interface may be developed to improve the selection, editing, and updating process of the estimated region. Moreover, during the manufacturing of the final prosthesis, minor inconsistencies in the estimation could be managed by blending it with the surrounding areas to create seamless boundaries at the prosthesis's edges.

As the method exclusively focuses on the outer surface, additional post-processing with software such as Mimics (Materialise, Leuven, Belgium) or Zbrush (Maxon, Los Angeles CA) is

required to construct a virtual prosthesis. This software enables the positioning of the prosthesis on the face, merging peripheries with scanned healthy tissue, and fitting it to the internal surface.

While our model significantly aids digital design, further refinement of the manufacturing workflow is needed to incorporate additional patient-specific data, enhancing customization and patient satisfaction. Our model is specifically designed for South African black adults and therefore has limited applicability to other demographics such as children or other ancestry groups. Future studies on other populations could assist in expanding the diversity of the sample population and therefore the wider applicability of such an SSM design. Finally, our model does not account for the forehead, ears, and occipital regions, as most CBCT scans do not capture these areas, limiting its comprehensiveness. These limitations underscore the need for further research to broaden the scope and accuracy of the facial prosthesis design process.

Though not the definitive model, the final estimation provided a realistic and precise depiction of the missing area, evidenced by acceptable RMS errors. The digital techniques we propose have the potential to reduce the dependence on artistic skills in the design and manufacture of facial prosthetics. Given the shortage of healthcare facilities and staff, 26–28 the implementation of automated and objective techniques may expand their availability and alleviate the workload of rehabilitation clinics.[54, 58] These advances could potentially enhance patient outcomes. Our research represents the initial stage in developing user-friendly software for 3D printing of a prosthetic model that fits the patient before the final silicone prosthesis is molded and cured. Indeed, given the rapid advancements in 3D printing technology, the prospect of directly printing the 3D prosthesis using silicone is becoming increasingly feasible.[59, 60]

CONCLUSION

The use of this statistical shape model has advantages over artistic and other computerized approaches for estimating missing soft tissue parts. In contrast to commonly employed artistic methods, the approach is objective, being derived from a statistical model of real facial variation. In contrast to mirroring approaches, it can be easily applied to defects crossing the midline and bilateral defects. This approach can help reduce the burden on rehabilitation clinics by assisting in faster and less laborious design and manufacture of aesthetic facial prostheses, ultimately aiding in improving the quality of life of patients, particularly those with midline or bilateral facial defects.

ACKNOWLEDGEMENTS

The authors want to thank the private healthcare providers at two private healthcare facilities for providing access to the scans at their departments. We would also like to thank Jack Qi for assistance with some of the graphical representations. Bakeng se Afrika (ERASMUS+ 597924-EPP-1-2018-1-ZA-EPPKA2-CBHE-J), an Erasmus+ (European Union) project.

CONFLICT OF INTEREST STATEMENT

The authors have no conflict of interest to declare.

REFERENCES

1. Bradbury E. Meeting the psychological needs of patients with facial disfigurement. *Br J Oral Maxillofac Surg*. 2012; 50(3): 193-196
2. Callahan C. Facial disfigurement and sense of self in head and neck cancer. *Soc Work Health Care*. 2005; 40(2): 73-87
3. Clarke A. 'What happened to your face?'Managing facial disfigurement. *Br J Community Nurs*. 1998; 3(1): 13-16
4. De Sousa A. Psychological issues in acquired facial trauma. *Indian J Plast Surg*. 2010; 43(2): 200-205
5. Jundt JS, Wong MEK, Tatara AM, Demian NM Invasive cutaneous facial mucormycosis in a trauma patient. *J Oral Maxillofac Surg*. 2018; 76(9): 1930.e1-1930.e5
6. Abdul Rahman N, Rajaratnam V, Burchell GL, Peters RMH, Zweekhorst MBM Experiences of living with leprosy: a systematic review and qualitative evidence synthesis. *PLoS Negl Trop Dis*. 2022; 16(10):e0010761
7. Zwane NB, Mohangi GU, Shangase SL. Head and neck cancers among HIV-positive patients: a five year retrospective study from a Johannesburg hospital, South Africa. *SADJ*. 2018; 73(3): 121-126
8. Feller L, Altini M, Chandran R, Khammissa RAG, Masipa JN, Mohamed A, Lemmer J Noma (cancrum oris) in the South African context. *J Oral Pathol Med*. 2014; 43(1): 1-6
9. Pedro K, Smit DA, Morkel JA. Cancrum Oris (noma) in an HIV-positive adult: a case report and literature review. *SADJ*. 2016; 71(6): 248-252
10. 1Sykes LM, Essop RM. Combination intraoral and extraoral prosthesis used for rehabilitation of a patient treated for cancrum oris: a clinical report. *J Prosthet Dent*. 2000; 83(6): 0613-0616
11. Pham KT, Hotez PJ, Hamilton KL. Reconstructive surgery for the neglected tropical diseases: global gaps and future directions. *Plast Reconstr Surg Glob Open*. 2023; 11(5):e4987
12. Nogueira T, Adorno M, Mendonça E, Leles C. Factors associated with the quality of life of subjects with facial disfigurement due to surgical treatment of head and neck cancer. *Med Oral Patol Oral Cir Bucal*. 2018; 23(2): e1698-6946
13. Scolozzi P, Jaques B. Treatment of midfacial defects using prostheses supported by ITI dental implants. *Plast Reconstr Surg*. 2004; 114(6): 1395-1404
14. Smith RM, Byrne PJ. Reconstruction of the ear. *Facial Plast Surg Clin North Am*. 2019; 27(1): 95-104
15. Konofaos P, Wallace RD. Nose reconstruction. in: SR Thaller, ZJ Panthaki (eds): Tips and tricks in plastic surgery. Cham: Springer International Publishing, 2022, pp 273–282
16. Mussi E, Servi M, Facchini F, Carfagni M, Volpe Y. A computer-aided strategy for preoperative simulation of autologous ear reconstruction procedure. *Int J Interact Des Manuf*. 2021; 15(1): 77-80

17. Wang W, Shokri T, Vincent A, Vest A, Williams F, Ducic Y. Palatomaxillary obturation and facial prosthetics in head and neck reconstruction. *Facial Plast Surg*. 2020; 36(06): 715-721
18. Kantar RS, Alfonso AR, Diep GK, Berman ZP, Rifkin WJ, Diaz-Siso JR, et al. Facial transplantation: principles and evolving concepts. *Plast Reconstr Surg*. 2021; 147(6): 1022e-1038e
19. Federspil P, Federspil PA. Prosthetic management of craniofacial defects. *HNO*. 1998; 46(6): 569-578
20. Klimczak J, Helman S, Kadakia S, Sawhney R, Abraham M, Vest AK, Ducic Y. Prosthetics in facial reconstruction. *Craniomaxillofac Trauma Reconstr*. 2018; 11(1): 006-14
21. Salazar-Gamarra R, Binasco S, Seelaus R, Dib LL. Present and future of extraoral maxillofacial prosthodontics: cancer rehabilitation. *Front Oral Health*. 2022; 3: 112
22. Sykes L, Essop A, Sukha A. An 8-year assessment of maxillofacial prosthetic patients treated in a Department of Prosthetic Dentistry. *SADJ*. 2001; 56(4): 198-202
23. Adeola H, Afrogheh A, Hille J. The burden of head and neck cancer in Africa: the status quo and research prospects. *SADJ*. 2018; 73(8): 477-488
24. StatsSA. Mid-year population estimates. In: Statistics South Africa, (ed.). 2022.
25. Omar M. The incidence and management of traumatic facial injury: 854 patients in 4 months in Charlotte Maxeke Johannesburg Academic Hospital (CMJA), South Africa. *3rd Online Edition of European Conference on Otolaryngology and ENT*. 2020 Webinar.
26. Tsĭtã KPM, Owen CP. Analysis of the need for, and scope of training in, maxillo-facial prosthodontics in the South African dental technology programme. *SADJ*. 2017; 72(1): 16-21
27. Tiwari R, Bhayat A, Chikte U. Forecasting for the need of dentists and specialists in South Africa until 2030. *PLoS One*. 2021; 16(5):e0251238
28. Bhayat A, Chikte U. Human resources for oral health care in south africa: a 2018 update. *Int J Environ Res Public Health*. 2019; 16(10): 1668
29. Din T, Jamayet N, Rajion ZA, Luddin N, Abdullah JY, Abdullah AM, Yahya S. Design and fabrication of facial prostheses for cancer patient applying computer aided method and manufacturing (CADCAM). Translational Craniofacial Conference. 2016 Penang, Malaysia.
30. Ambellan F, Lamecker H, von Tycowicz C, Zachow S. Statistical shape models: understanding and mastering variation in anatomy. *Adv Exp Med Biol*. 2019; 115667-115684
31. Audenaert EA, Pattyn C, Steenackers G, De Roeck J, Vandermeulen D, Claes P. Statistical shape modeling of skeletal anatomy for sex discrimination: their training size, sexual dimorphism, and asymmetry. *Front Bioeng Biotechnol*. 2019; 7: 302
32. Meynen A, Matthews H, Nauwelaers N, Claes P, Mulier M, Scheys L. Accurate reconstructions of pelvic defects and discontinuities using statistical shape models. *Comput Methods Biomech Biomed Engin*. 2020; 23(13): 1026-1033
33. Raith S, Wolff S, Steiner T, Modabber A, Weber M, Hölzle F, Fischer H. Planning of mandibular reconstructions based on statistical shape models. *Int J Comput Assist Radiol Surg*. 2017; 12(1): 99-112
34. Gass M, Füßinger MA, Metzger MC, Schwarz S, Bähr JD, Brandenburg LS, et al. Virtual reconstruction of orbital floor defects using a statistical shape model. *J Anat*. 2022; 240(2): 323-329

35. Fuessinger MA, Schwarz S, Cornelius C-P, Metzger MC, Ellis E, Probst F, et al. Planning of skull reconstruction based on a statistical shape model combined with geometric morphometrics. *Int J Comput Assist Radiol Surg*. 2017; 13: 519-529
36. Fuessinger MA, Schwarz S, Neubauer J, Cornelius C-P, Gass M, Poxleitner P, et al. Virtual reconstruction of bilateral midfacial defects by using statistical shape modeling. *J Craniomaxillofac Surg*. 2019; 47(7): 1054-1059
37. White JD, Ortega-Castrillón A, Matthews H, Zaidi AA, Ekrami O, Snyders J, et al. MeshMonk: open-source large-scale intensive 3D phenotyping. *Sci Rep*. 2019; 9(1): 6085
38. MATLAB. (ed 9.11.0.1837725 (2021b)). Natick, Massachusetts, The Mathworks, Inc., 2021.
39. Marzola A, Robilotta C, Volpe Y, Governi L, Furferi R. Statistical shape model: comparison between ICP and CPD algorithms on medical applications. *Int J Interact Des Manuf*. 2021; 15: 85-89
40. Kuznetsova A, Brockhoff P, Christensen R. lmerTest package: tests in linear mixed effect models. *J Stat Softw*. 2017; 821-826
41. Core Team R. R: A language and environment for statistical computing. Vienna, Austria: R Foundation for Statistical Computing, 2022.
42. Choi JW, Lee JY, Oh T-S, Kwon SM, Yang SJ, Koh KS. Frontal soft tissue analysis using a 3 dimensional camera following two-jaw rotational orthognathic surgery in skeletal class III patients. *J Craniomaxillofac Surg*. 2014; 42(3): 220-226
43. Jiao T, Zhang F, Huang X, Wang C. Design and fabrication of auricular prostheses by CAD/CAM system. *Int J Prosthodont*. 2004; 17(4): 460-463
44. Miechowicz S, Wojnarowska W, Majkut S, Trybulec J, Pijanka D, Piecuch T, et al. Method of designing and manufacturing craniofacial soft tissue prostheses using Additive Manufacturing: a case study. *Biocybern Biomed Eng*. 2021; 41(2): 854-865
45. Sherwood RG, Murphy N, Kearns G, Barry C. The use of 3D printing technology in the creation of patient-specific facial prostheses. *Ir J Med Sci*. 2020; 189(4): 1215-1221
46. Subburaj K, Nair C, Rajesh S, Meshram SM, Ravi B. Rapid development of auricular prosthesis using CAD and rapid prototyping technologies. *Int J Oral Maxillofac Surg*. 2007; 36(10): 938-943
47. Sun J, Xi J, Chen X, Xiong Y. A CAD/CAM system for fabrication of facial prostheses. *Rapid Prototyp J*. 2011; 17(4): 253-261
48. Sun M-H, Yen C-H, Tsai Y-J, Liao Y-L, Wu S-Y. Fabrication of a facial prosthesis for a 13-year-old child by using a point-and-shoot three-dimensional scanner and CAD/CAM technology. *Taiwan J Ophthalmol*. 2022; 12(2): 219-222
49. Verdonck HW, Poukens J, Overveld HV, Riediger D. Computer-assisted maxillofacial prosthodontics: a new treatment protocol. *Int J Prosthodont*. 2003; 16(3): 326-328
50. Abdulameer HM, Tukmachi M. Nasal prosthesis fabrication using rapid prototyping and 3D printing (A case study). *Int J Innov Res Sci Eng Technol*. 2016; 6(8): 15520-15526
51. Bi Y, Wei H. Fully digital workflow for the rehabilitation of a total nasal defect with a prosthesis. *J Prosthet Dent*. 2022. https://doi.org/10.1016/j.prosdent.2022.03.012
52. Palousek D, Rosicky J, Koutny D. Use of digital technologies for nasal prosthesis manufacturing. *Prosthet Orthot Int*. 2014; 38(2): 171-175
53. Sun J, Chen X, Liao H, Xi J. Template-based framework for nasal prosthesis fabrication. *Rapid Prototyp J*. 2013; 19(2): 68-76

54. Tetteh S, Bibb RJ, Martin SJ. Maxillofacial prostheses challenges in resource constrained regions. *Disabil Rehabil*. 2019; 41(3): 348-356
55. Van Heerden I, Fossay A. Changing world of external maxillofacial prosthesis manufacturing. 20th Annual International RAPDASA Conference. 2019 Bloemfontein, South Africa.
56. Mohammed MI, Cadd B, Peart G, Gibson I. Augmented patient-specific facial prosthesis production using medical imaging modelling and 3D printing technologies for improved patient outcomes. *Virtual Phys Prototy*. 2018; 13(3): 164-176
57. Sarkar MA, Chahar MP, Gowda BEM, et al. Prosthetic rehabilitation of an orbital defect using computer aided designing and rapid prototyping. *Int J Contemp Med Res*. 2019; 6(1): A15-A17.
58. Slijepcevic AA, Afshari A, Vitale AE, Couch SM, Jeanpierre LM, Chi JJ. A contemporary review of the role of facial prostheses in complex facial reconstruction. *Plast Reconstr Surg*. 2023; 151(2): 288e-298e.
59. Fay CD, Jeiranikhameneh A, Sayyar S, Talebian S, Nagle A, Cheng K, et al. Development of a customised 3D printer as a potential tool for direct printing of patient-specific facial prosthesis. *Int J Adv Manuf Tech*. 2022; 120(11-12): 7143-7155
60. Unkovskiy A, Spintzyk S, Brom J, Huettig F, Keutel C. Direct 3D printing of silicone facial prostheses: a preliminary experience in digital workflow. *J Prosthet Dent*. 2018; 120(2): 303-308.
61. Jurić B, Matijaš T. The role of CBCT in the field of dental implantology. *Radiološki Vjesnik*. 2023; 47(1): 16-27.